Cell Reports, Volume *32*

Supplemental Information

In Vivo Chimeric Alzheimer's Disease Modeling of Apolipoprotein E4 Toxicity in Human Neurons

Ramsey Najm, Kelly A. Zalocusky, Misha Zilberter, Seo Yeon Yoon, Yanxia Hao, Nicole Koutsodendris, Maxine Nelson, Antara Rao, Alice Taubes, Emily A. Jones, and Yadong Huang

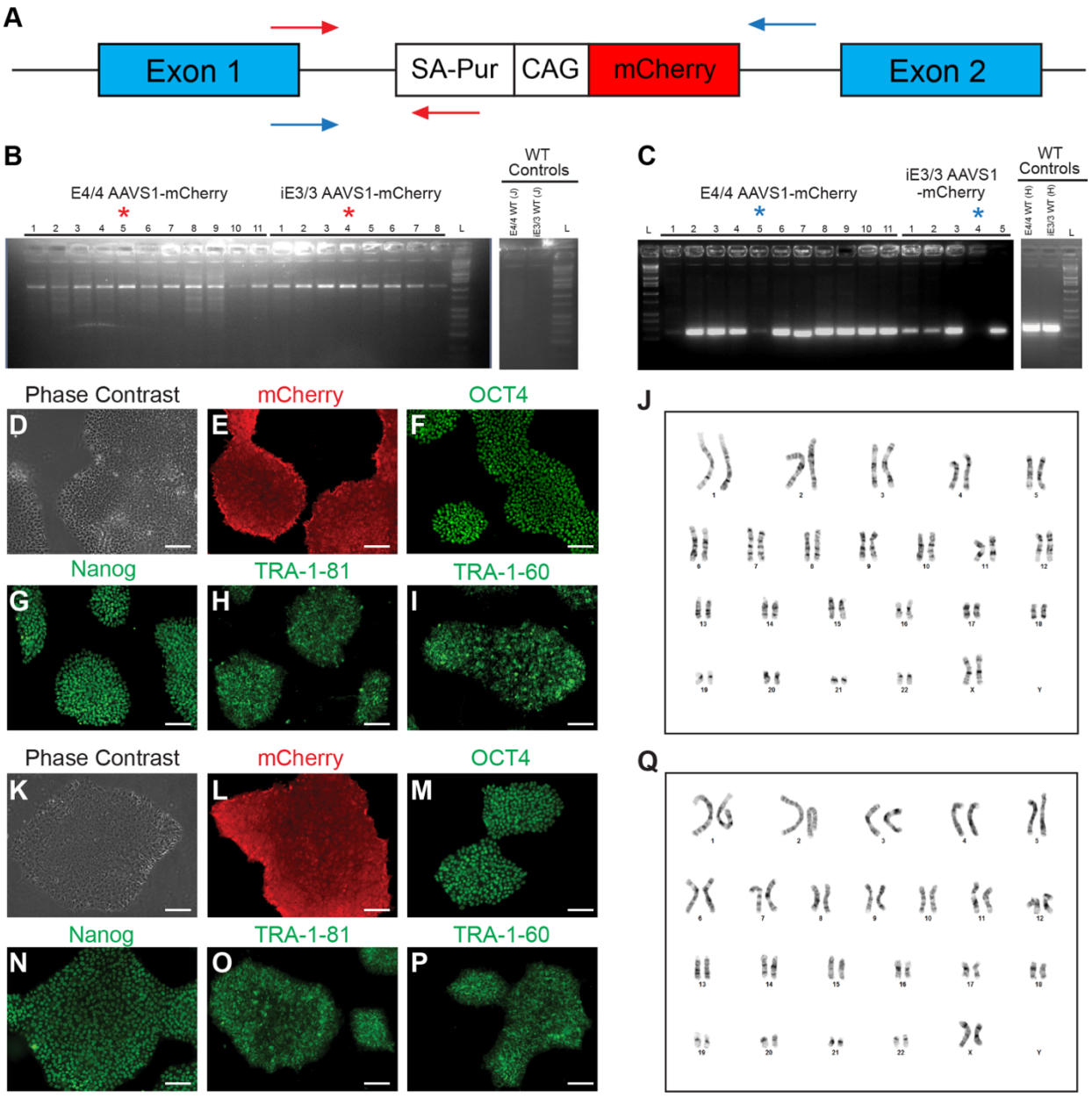

Figure S1. Genotyping validation and characterization of AAVS1-mCherry E4/4-hiPSC and iE3/3-hiPSC lines. Related to Figure 1.

(A) Construct and genotyping strategy for *AAVS1* targeting of the mCherry transgene expression cassette. The red arrows and blue arrows indicate PCR primers for *AAVS1* locus insertion or homozygosity, respectively.

(B and C) PCR genotyping of mCherry-containing hiPSC clones. The expected PCR products for correctly targeted *AAVS1* locus are ~1000bp (B). Two selected clones with a red asterisk underwent a further homozygosity assay and clones with the PCR products of ~650bp are heterozygous and the clones without PCR products are homozygous (blue asterisk).

(D) Phase contrast image of the homozygous AAVS1-mCherry^{+} iE3/3-hiPSC Clone 4. Scale bar, 100μm.

(E–I) Immunocytochemical staining for mCherry (E) and classical pluripotency markers (F–I) in the homozygous AAVS1-mCherry^{+} iE3/3-hiPSC Clone 4. Scale bar, 100μm**.**

(J) Karyotype of the homozygous AAVS1-mCherry^{+} iE3/3-hiPSC Clone 4.

(K) Phase contrast image of the homozygous AAVS1-mCherry^{+} E4/4-hiPSC Clone 5. Scale bar, 100μm.

(L–P) Immunocytochemical staining for mCherry (L) and classical pluripotency markers (M–P) in homozygous AAVS1-mCherry^{+} E4/4-hiPSC Clone 5. Scale bar, 100μm.

(Q) Karyotype of the homozygous AAVS1-mCherry^{+} E4/4-hiPSC Clone 5.

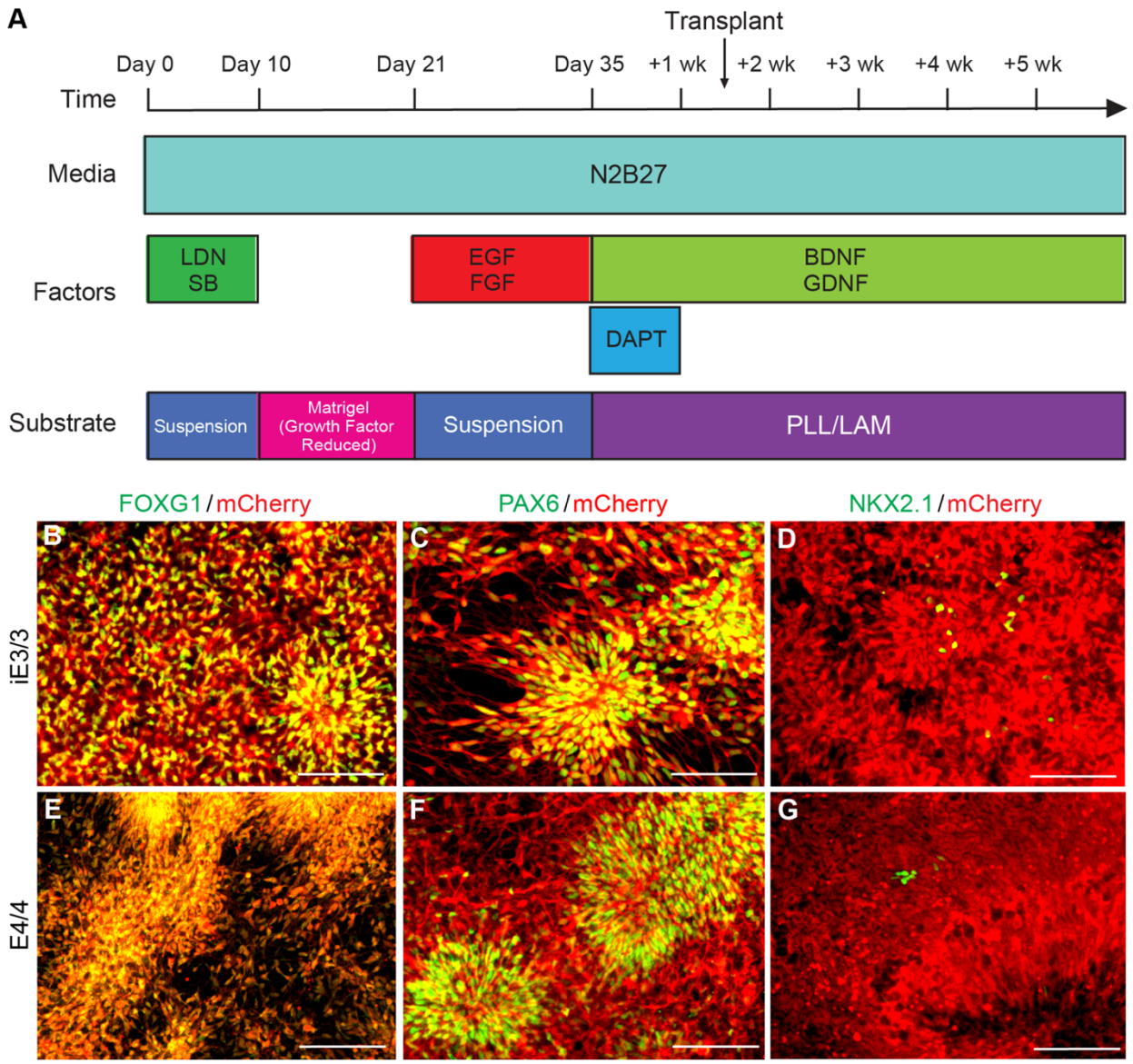

Figure S2. Validation of hiPSC-derived neuronal progenitor lineages. Related to Figure 2.

(A) Schematic of neuronal differentiation strategy. Transplantation was performed when neurons were between +1 week (wk) and +2 weeks of maturation.

(B–D) Immunostaining of iE3/3-mCherry neuronal progenitors at day 21 for classical markers of the telencephalon (FOXG1), dorsal cortical progenitors (PAX6), and the MGE (NKX2.1). Scale bar, 100μm.

(E–G) Immunostaining of E4/4-mCherry neuronal progenitors at day 21 for classical markers of the telencephalon (FOXG1), dorsal cortical progenitors (PAX6), and the MGE (NKX2.1). Scale bar, 100μm.

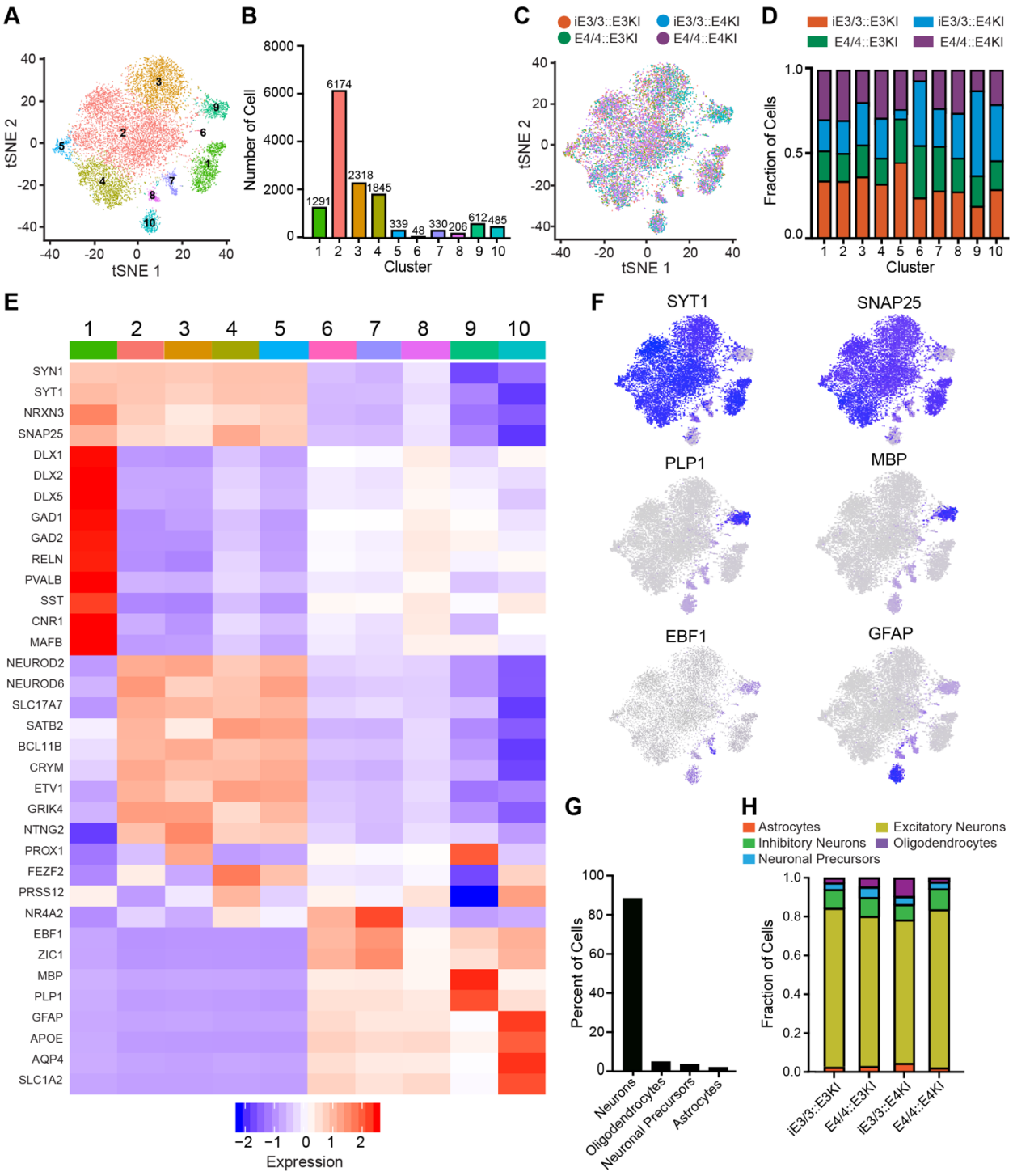

Figure S3. Lineage validation of transplanted human cells based on gene expression profile derived from snRNA-seq. Related to Figure 3.

(A) tSNE clustering of transplanted human cells at 7 months post-transplantation. Cluster 1: inhibitory neurons, Clusters 2–5: excitatory neurons, Clusters 6–8: neuronal progenitors, Cluster 9: oligodendrocytes, Cluster 10: astrocytes.

(B) Quantification of the number of cells per cluster in the transplanted cells.

(C) tSNE clustering of transplanted human cells grouped by sample.

(D) Quantification of the fraction of cells from each sample per cluster.

(E) Heatmap displaying genes representative of lineages present in transplanted human cells.

(F) Feature plots displaying the distribution of classical markers of lineages present in transplanted human cells.

(G) Quantification of the percent of cell lineages from all transplants combined.

(H) Quantification of the fraction of cell types present within each transplantation group.

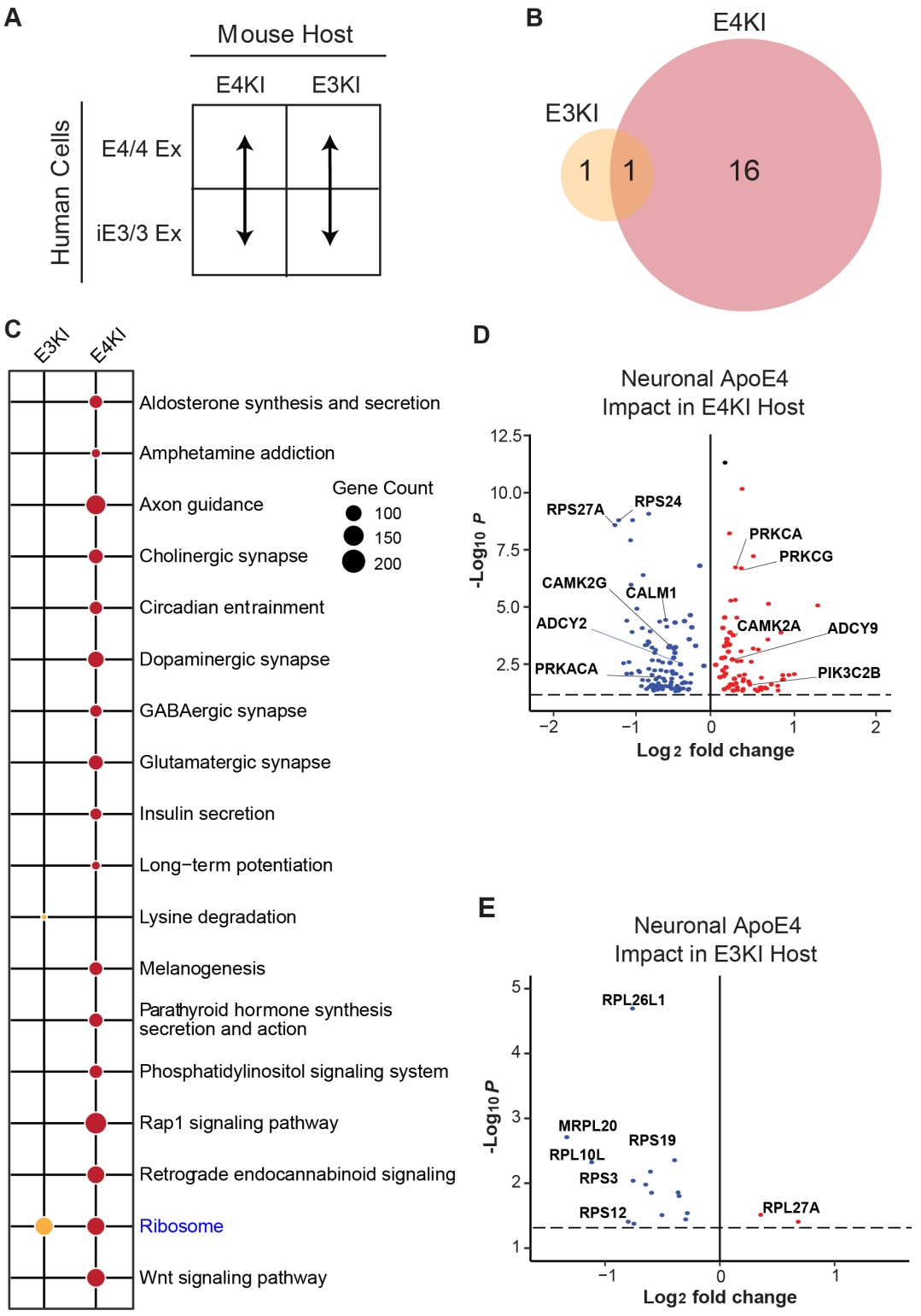

Figure S4. Differential responses of human excitatory neurons to neuronally produced (endogenous) apoE3 and apoE4. Related to Figure 4.

(A) These comparisons were made between E4/4- and iE3/3-hiPSC-derived human excitatory neurons within apoE-genotype-matched mouse hosts. Ex denotes excitatory neurons.

(B) Many more pathways were dysregulated by transplanted excitatory neuronal apoE4 genotype in the E4KI mouse host environment than in the E3KI mouse host environment.

(C) Dotplot indicating the pathways dysregulated by transplanted excitatory neuron apoE4 genotype in the E4KI mouse host environment and in the E3KI mouse host environment. Node size indicates the number of genes dysregulated within the pathway. Shared pathways are highlighted in blue.

(D and E) Genes dysregulated by transplanted human excitatory neuron apoE4 genotype in the E4KI mouse environment (D) and in the E3KI mouse environment (E). Red points represent an increase in Log_2 fold change and blue points represent a decrease in Log_2 fold change in response to neuronal apoE4. Only genes with a Benjamini-Hochberg corrected $p < 0.05$ are shown. P-values are assigned on a per-cell basis.

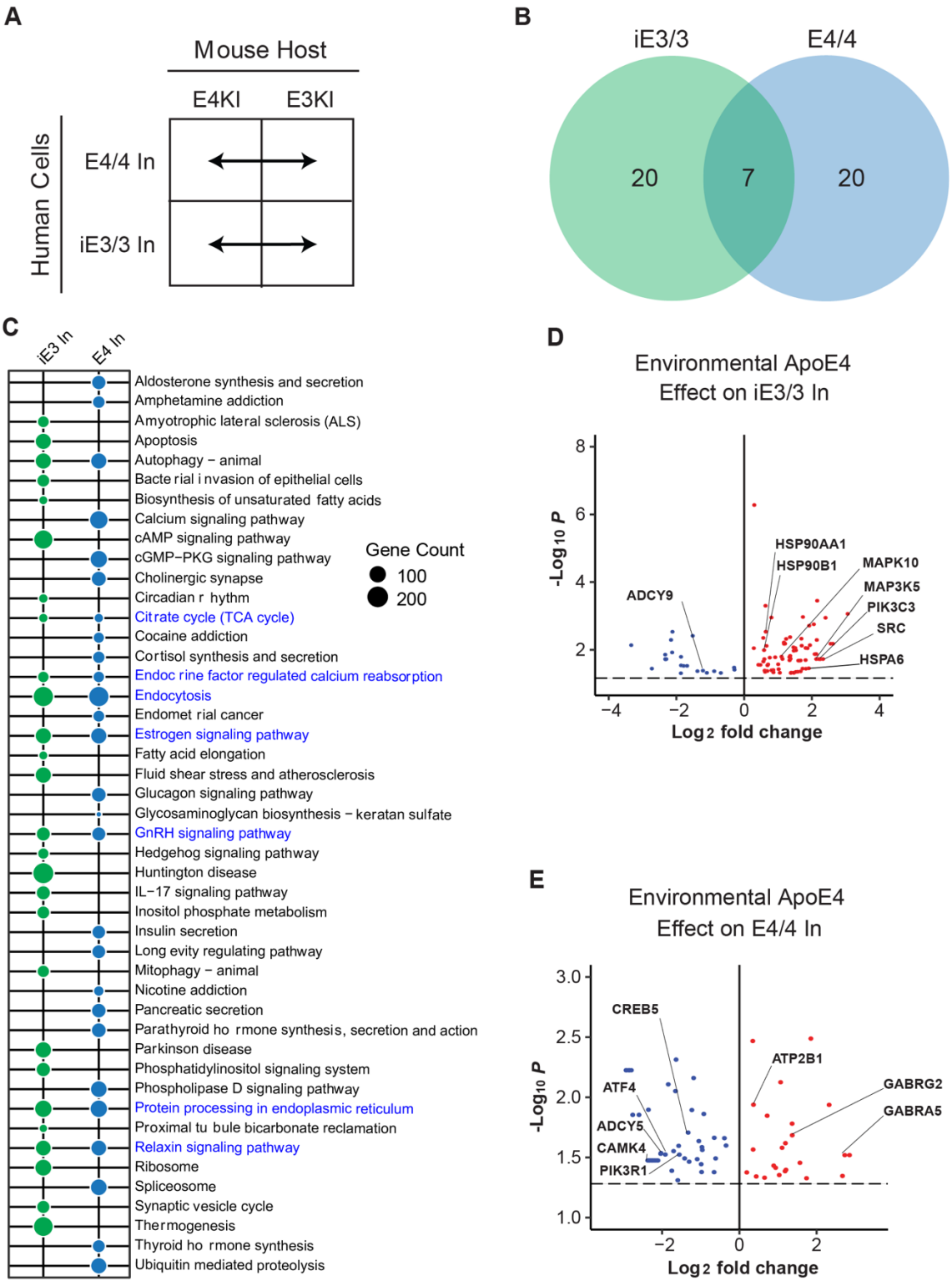

Figure S5. Differential responses of iE3/3 and E4/4 human inhibitory neurons to environmental (exogenous) apoE4. Related to Figure 5.

(A) These comparisons were made for apoE-genotype-matched hiPSC-derived human inhibitory neurons across E4KI and E3KI mouse hosts.

(B) The number of pathways dysregulated by the E4KI mouse host environment was equal in E4/4 hiPSC-derived human inhibitory neurons and in iE3/3 hiPSC-derived human inhibitory neurons.

(C) Dotplot indicating the pathways dysregulated by the E4KI mouse host environment in E4/4 hiPSC-derived human inhibitory neurons and in iE3/3 hiPSC-derived human inhibitory neurons. Node size indicates the number of genes dysregulated within the pathway. Shared pathways are highlighted in blue.

(D and E) Genes dysregulated by the E4KI mouse environment in iE3/3 hiPSC-derived human inhibitory neurons (D) and in E4/4 hiPSC-derived human inhibitory neurons (E). Red points represent an increase in Log_2 fold change and blue points represent a decrease in Log_2 fold change in response to the E4KI brain environment. Only genes with a Benjamini-Hochberg corrected $p < 0.05$ are shown. P-values are assigned on a per-cell basis.

In panels A, C, D, and E, In denotes inhibitory neurons.

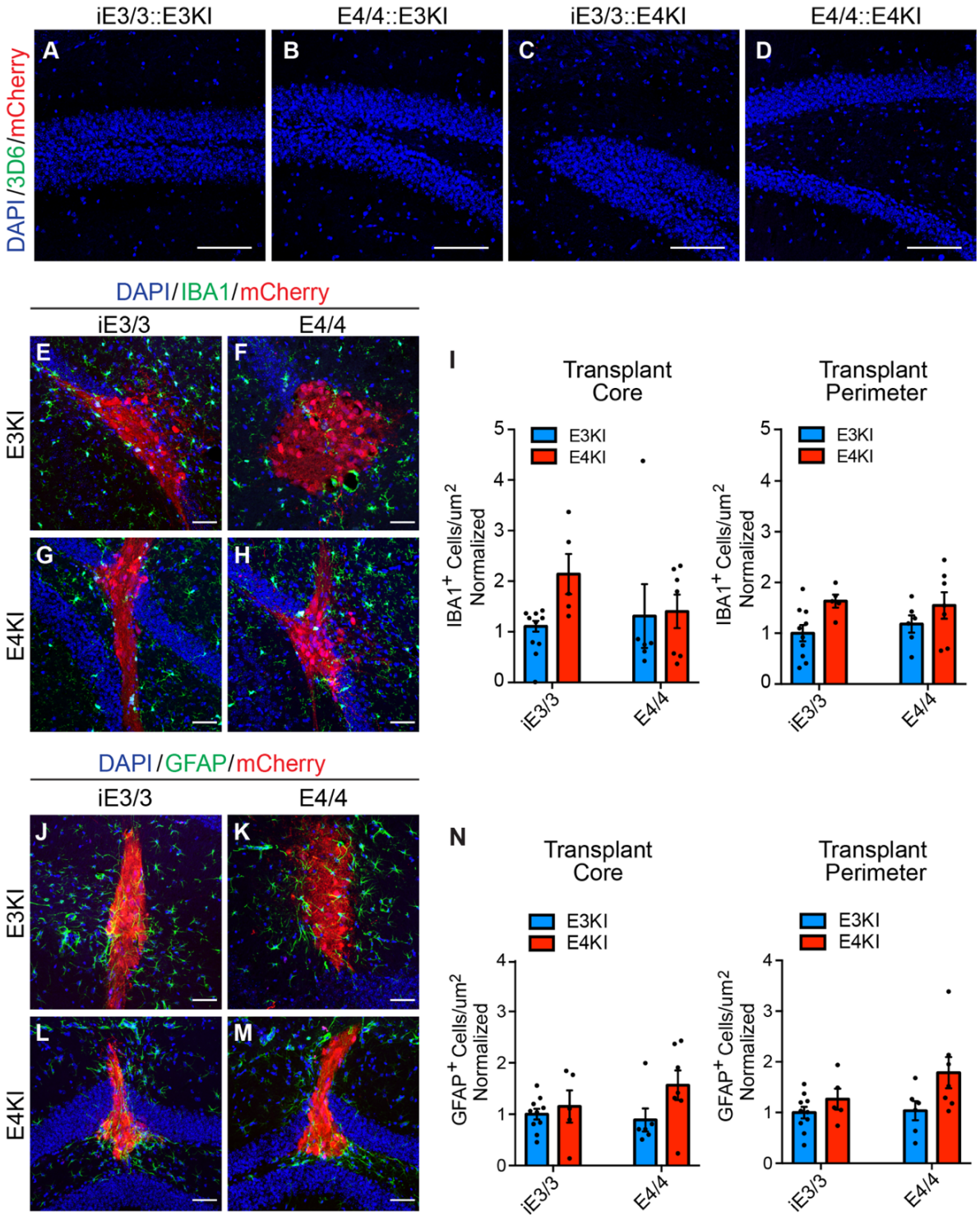

Figure S6. Contribution of mouse cells to Aβ staining and response of mouse glial cells to hiPSC-derived neuron transplants. Related to Figures 6 and 7.

(A–D) Immunohistochemical staining of Aβ (green) in regions distal to the transplant core. Note that in the region where there were no mCherry^{+} (red) human neurons, there was no 3D6^{+} Aβ staining. Scale bar, 100μm.

(E–H) Immunohistochemical staining of IBA1$^+$ (green) mouse microglia in and on the perimeter of the mCherry$^+$ (red) human neuronal transplants. Scale bar, 50μm.

(I) Quantification of the number of IBA1$^+$ mouse microglia per area within the mCherry$^+$ human neuronal transplants (left) and number of IBA1$^+$ mouse microglia per area on the perimeter of the mCherry$^+$ human transplants (right). Values are normalized to the E3KI brain transplanted with iE3/3-neurons (E3KI: iE3/3 transplants, n = 10, N = 3; E4/4 transplants, n = 6, N = 3. E4KI: iE3/3 transplants, n = 5, N = 3; E4/4 transplants, n = 7, N = 3). Data are represented as Mean ± SEM, two-way ANOVA with Sidak's multiple comparisons test.

(J–M) Immunohistochemical staining of GFAP$^+$ (green) mouse astrocytes in and on the perimeter of the mCherry$^+$ (red) human neuronal transplants. Scale bar, 50μm.

(N) Quantification of the number of GFAP$^+$ mouse astrocytes per area within the mCherry$^+$ human neuronal transplants (left) and number of GFAP$^+$ mouse astrocytes per area on the perimeter of the mCherry$^+$ human neuronal transplants (right). Values are normalized to the E3KI brain transplanted with iE3/3-neurons (E3KI: iE3/3 transplants, n = 10; E4/4 transplants, n = 6. E4KI: iE3/3 transplants, n = 5; E4/4 transplants, n = 7). Data are represented as Mean ± SEM, two-way ANOVA with Sidak's multiple comparisons test.